

<https://doi.org/10.1038/s43247-024-01937-z>

# Global warming may turn ice-free areas of Maritime and Peninsular Antarctica into potential soil organic carbon sinks



Danilo C. de Mello<sup>1,2</sup>, Márcio R. Francelino<sup>1,2</sup>✉, Cássio M. Moquedace<sup>1,2</sup>, Clara G. O. Baldi<sup>1,2</sup>, Lucas V. Silva<sup>1,2</sup>, Rafael G. Siqueira<sup>1,2</sup>, Gustavo V. Veloso<sup>1,2</sup>, Elpidio I. Fernandes-Filho<sup>1,2</sup>, André Thomazini<sup>3</sup>, José A. M. Demattê<sup>4</sup>, Tiago O. Ferreira<sup>4,5</sup>, Lucas Carvalho Gomes<sup>6</sup>, Eduardo O. Senra<sup>7</sup> & Carlos E. G. R. Schaefer<sup>1,2</sup>

The impact of intensified climate change driven by global warming on the stocks and dynamics of soil organic carbon in Antarctica is currently uncertain. Our objective with this was evaluate the potential repercussions of global warming on soil organic carbon under three Shared Socioeconomic Pathways. Employing a methodology that integrates soil field data, machine learning, and projections of future climate change scenarios for the Maritime and Peninsular Antarctic ice-free areas, we focus on predicting the soil organic carbon within the 0–30 cm soil layer. To achieve this, we utilized one of the largest soil databases of Antarctica, which contains data from 2800 observation sites. In our predictive modeling of SOC stocks, we used relief data and, bioclimatic variables (from Chelsa database) as predictor variables, primarily focusing on temperature, precipitation, and net primary production. The prediction performance of the soil organic carbon stocks model, as measured by concordance correlation coefficient, was 0.52 for the 0–5 cm soil depth, 0.56 for the 5–15 cm depth, and 0.46 for the 15–30 cm depth. Our model reveal that the effects of climate change, primarily changes in temperature and precipitation, are going to increase in soil organic carbon stock ( $359 \pm 146$  Mg to  $686 \pm 197$  Mg), indicating that ice-free regions of Maritime and Peninsular Antarctica will tend to function as a carbon sink. However, the magnitude of the soil carbon sink is contingent upon the existing soil organic carbon content and soil depth. The estimated soil organic carbon stocks are controlled mainly by temperature and precipitation, which are interconnected with net primary productivity.

The islands of Maritime Antarctica (MA), including South Shetlands have shown some of the fastest warming rates measured in the Southern Hemisphere<sup>1</sup>. In addition, the Eastern Antarctic Peninsula (AP), is among the regions worldwide experiencing the most rapid warming<sup>2</sup>. Previous research suggested that AP region can serve as a terrestrial carbon sink<sup>3</sup>, due to recent colonization by plant communities exhibiting efficient net primary production (NPP), significant carbon input and soil carbon storage<sup>4–6</sup>. Despite the well-documented soil organic carbon (SOC) stocks in the Arctic terrestrial ecosystems, uncertainties persist regarding the precise SOC stock in Antarctica. Recent studies have already evaluated carbon cycle feedbacks

from the warming Arctic permafrost under climate change scenarios<sup>7</sup>. However, it remains unclear whether Antarctic soils will act as a carbon sink or source under the Intergovernmental Panel on Climate Change (IPCC) projections, which indicate global average temperatures could rise by more than 1.5 °C in the medium to long term.

The main contributions to SOC in Antarctic soils include various sources such as microorganisms such as cyanobacteria and blue-green algae<sup>8</sup>, and fungi<sup>9</sup>, which are capable of surviving in extreme conditions and play a crucial role in the production and decomposition of organic matter<sup>10</sup>. Although limited in a number of species, lichens and mosses significantly

<sup>1</sup>Laboratório de Pedometria e Geoprocessamento (LabGeo), Universidade Federal de Viçosa, Viçosa, Brazil. <sup>2</sup>Department of Soil Science, Universidade Federal de Viçosa, Viçosa, Brazil. <sup>3</sup>Center of Agrarian Sciences, Universidade Federal de São João Del-Rei, Sete Lagoas, Minas Gerais, Brazil. <sup>4</sup>Department of Soil Science, Luiz de Queiroz College of Agriculture, University of São Paulo, Piracicaba, Brazil. <sup>5</sup>Center for Carbon Research in Tropical Agriculture (CCARBON), University of São Paulo (USP), 13418900 Piracicaba, Brazil. <sup>6</sup>Department of Agroecology, Aarhus University, Aarhus, Denmark. <sup>7</sup>Instituto de Ciências Agrárias, Universidade Federal de Uberlândia, Campus Monte Carmelo, Uberlândia, Brazil. ✉e-mail: [marcio.francelino@ufv.br](mailto:marcio.francelino@ufv.br)

contribute to soil organic carbon in Antarctica<sup>11</sup>. In Antarctica, these organisms decompose very slowly due to low temperatures, allowing carbon to accumulate in the soil. In some coastal areas, deposits of organic material can come from marine sources like seaweed washed ashore and marine bird droppings (guano) deposits (such as penguin rookeries), which are rich in organic carbon and nutrients<sup>4</sup>. The non-vascular plants like moss cover can driver of accumulation of SOC in soils of particular Antarctic places like Victoria Land<sup>12</sup>. Also, the two native vascular plant species, *Deschampsia antarctica* and *Colobanthus quitensis*, although limited in distribution, also contribute to SOC through the deposition of their plant residues<sup>13</sup>, which are decomposed by microorganisms. Additionally, organic material can be transported to Antarctica through air currents<sup>14</sup>. This material includes spores, pollen, and small fragments of plants from other parts of the world.

Predicting and quantifying variations in SOC stocks in Antarctica under different climate change scenarios presents significant challenges. This is primarily due to the challenges of obtaining spatiotemporal data from the harsh and inaccessible ice-free areas of the continent<sup>15</sup>, the high cost and time demands of fieldwork, the significant spatial heterogeneity of Antarctic environments, and the reduced soil carbon responses to climate variation caused by pedological processes<sup>16</sup>.

There are currently no predictive models available for estimating the quantity of carbon likely to be stored in Antarctic soils across various soil depths and, landscapes and under different climate scenarios. Nevertheless, investigations on the distribution of SOC have been undertaken through diverse approaches elsewhere in the world, mainly through the application of machine learning (ML) techniques and the spatial relationships of the environmental factors<sup>17,18</sup>. In addition, recent research has been conducted with the objective to predict SOC stocks over time and assess their correlation with climate change<sup>19,20</sup>. However, most of these studies were conducted in Arctic soil environments<sup>7,21,22</sup>, with fewer studies focusing on Antarctic soils in the context of global warming. This is primarily due to the limited availability of soil data and the complexity of the Antarctic continent<sup>23</sup>, as well as the insufficient representation of Antarctic soils in global soil databases<sup>16</sup>.

Even in the most advanced and recent studies modeling major soil chemical properties in some ice-free areas of Antarctica<sup>16</sup>, predicting SOC stocks remains a significant gap that still awaits comprehensive exploration and mapping<sup>24,25</sup>. Moreover, the potential for current ice-free areas in Antarctica to increase SOC stocks in future climate change scenarios remains uncertain<sup>4</sup>. Uncertainties associated with insufficient information persist regarding the dynamics of SOC in Antarctica. Addressing such knowledge gaps can significantly contribute to global warming mitigation strategies by informing Antarctic conservation efforts and environmental management initiatives. Additionally, it can enhance the accuracy of long-term predictions in current climate change models.

Here, our objective was to estimate the dynamics of SOC stocks at various soil depths in the present time and under three different future climate change scenarios for the 0–30 cm soil layer. Additionally, we aimed to evaluate whether the soil in ice-free areas of MA and the AP, which have distinct climatic conditions, acts as a source or sink for atmospheric carbon. To achieve these goals, we utilized climate data from Chelsa under the IPCC global scenarios, incorporating topographic variables and, net primary production, and employed machine learning techniques. Three Shared Socioeconomic Pathways (SSPs) were considered in the predictive model.

## Results

### Predicted SOC stock at the present time in MA and AP

The estimated SOC stock maps illustrate variations in carbon stock, ranging from 0.56 to 19.27 Mg ha<sup>-1</sup> across three soil depths and eighteen different islands in the MA and AP regions, including James Ross Island (Fig. 1). In the first SOC stock map (Fig. 1), our model demonstrates the SOC stock at the present time. Consequently, our values and the spatial distribution of SOC stocks reflect only the estimated conditions of the present moment. Also, the SOC stock values are related to the existing climate gradient in the study area, wherein islands situated towards the edges of the continent experience higher temperatures and humidity (consequently greater SOC

stock values), while those closer to the peninsula exhibit lower temperatures and precipitation (lower SOC stock values) (Fig. 1). The variations in the estimated levels of SOC stocks also varied in response to soil depths. Notably, the surface soil layer exhibited the highest estimated SOC values, while the deeper layers presented comparatively smaller values (Fig. 1). The total estimated carbon stocks, categorized by island, indicated that James Ross Island had the highest estimated SOC values, while Barrientos had the lowest (Fig. 1). The average SOC stocks may not correspond directly to total carbon stocks, as shown by the different ranking of islands based on average versus total SOC values (both ranked from highest to lowest) (Fig. 1). For example, Ardley Island has the highest estimated average SOC but the lowest total stock due to its small size, making it less significant in terms of total SOC. Conversely, James Ross Island (JRI), with a low average SOC, ranks high in total SOC because of its large size and greater representation in the study area (Fig. 1).

### SOC responses to global warming in different scenarios in MA and AP

Our model estimated a substantial increase of SOC stocks for all three SSP scenarios (Fig. 2). While the SOC increments exhibit a directly proportional relationship with temperature increases across the entire region according to the SSP scenarios, some islands show a decrease in SOC stocks. Initially, we analysed the overall regional trends, followed by a closer examination of individual islands (Fig. 2). Under SSP1-2.6 (1.5 °C warming), SOC stocks increase by 27.67% compared to present levels. In SSP3-7.0 and SSP5-8.5 (2.5 °C and 4 °C warming), SOC stocks increase more substantially by 53.34% and 52.89%, respectively (see quantile 0.5, Fig. 1, supplementary information). This corresponds to increases in SOC stocks at 0–30 cm soil depth ranging from 17.22 to 51.07 Mg ha<sup>-1</sup> in SSP1-2.6, 24.58 to 61.48 Mg ha<sup>-1</sup> in SSP3-7.0, and 23.54 to 59.57 Mg ha<sup>-1</sup> in SSP5-8.5. Thus, due to the increase in temperature and precipitation estimated in the IPCC global scenarios, the values of SOC stocks are expected to increase across all three soil depths modelled in this work. Nevertheless, the increase in SOC stocks vary in proportion across the different soil layers, decreasing with depth (Fig. 2, supplementary information).

The quantities of SOC stocks estimated by our model also varied according to the different islands mapped (Fig. 2). Significantly, most areas are estimated to experience an increase SOC stocks, particularly Deception, Livingston and James Ross Island. In contrast, Nelson Island, Hope Bay, and Snow Hill Island are estimated to experience a decrease SOC stocks. It is important to highlight that the variations in SOC stocks per island may not offer a representative portrayal of the entire ice-free area. For instance, even if the contributed values for a particular island are substantial, the significance of these values can be diminished by the small size of the island relative to the overall study area.

### Environmental drivers of the responses of SOC to global warming

The control over changes to the SOC stock, considering the three SSPs global warming scenarios (SSP1-2.6, SSP3-7.0, and SSP5-8.5), is predominantly regulated by four environmental variables, which contribute to our predictive modelling by ~75%—precipitation of the driest month, precipitation seasonality, ridge level, and precipitation of the wettest month (BIO 14, BIO 15, Ridge Level, and BIO 13, respectively) (Fig. 3). Additionally, the responses of SOC stock to warming scenarios are influenced by annual precipitation, temperature seasonality, and annual mean temperature (BIO 12, BIO 4, and BIO 1, respectively), contributing close to 50% (Fig. 3) to the response. The selection of environmental variables in predicting SOC stocks was performed based on their importance using the recursive feature elimination (RFE) algorithm (Methods section). This algorithm systematically eliminates the least promising environmental predictor variables from the model based on an initial measure of predictor importance, thereby generating a most parsimonious model for explaining SOC stock predictions. The RFE method provided a significant reduction of variables combined with satisfactory performance in the predicting SOC stocks influenced by various global warming scenarios across distinct soil

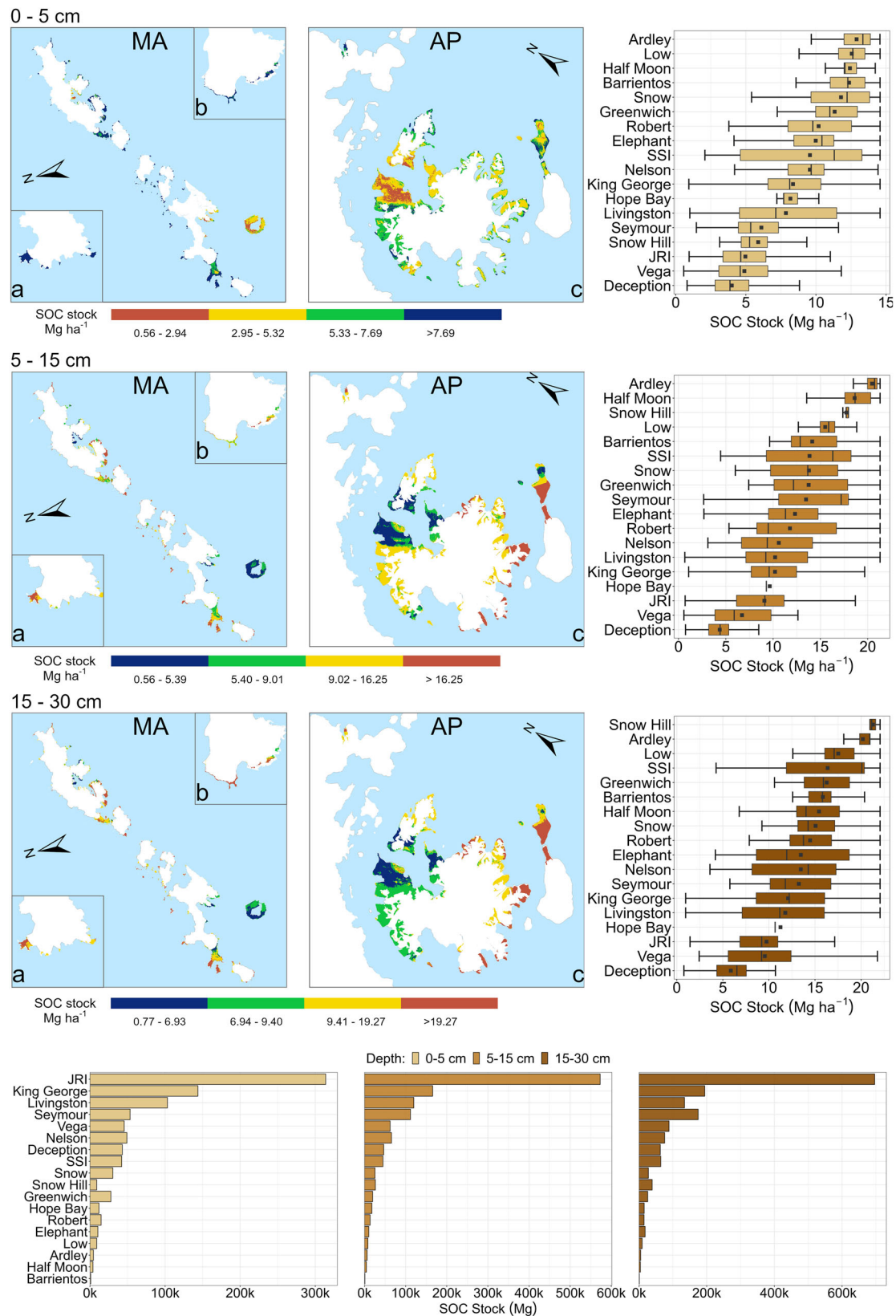


**Fig. 1 | Predicted SOC stock maps for MA and the AP at the present time.** The South Shetland Islands are portrayed at the centre of the left squares, including **a:** Low Island and **b:** Elephant Island. In the right squares, **c:** the James Ross, Vega, Seymour, and Snow Hill Islands are represented. On the right, boxplots illustrate

variations in estimated SOC stock levels (average, maximum, and minimum) across different islands within the study area and at various depths. The bar charts at the bottom represents estimated total carbon stocks categorized by island.

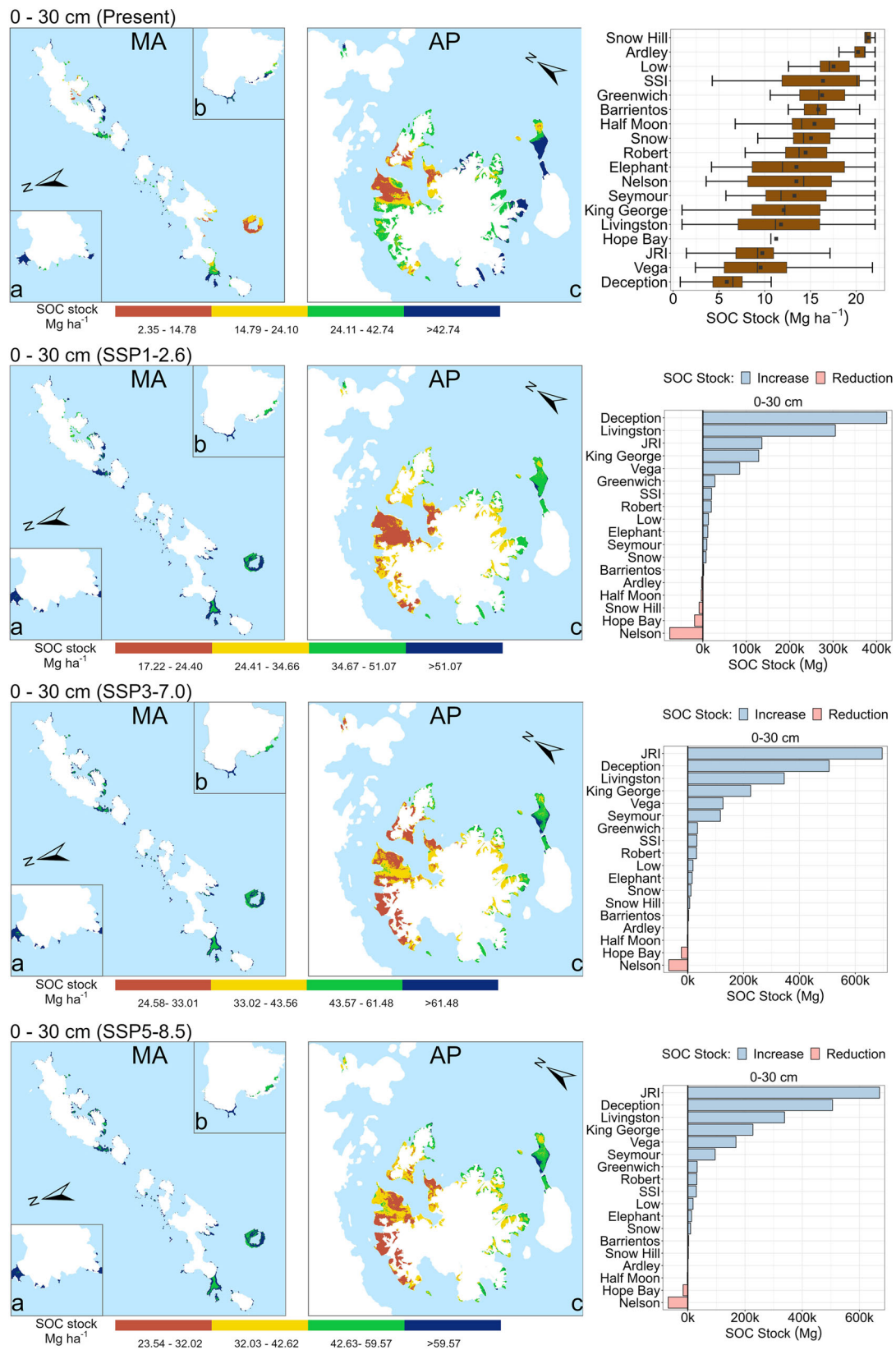


**Fig. 2 | Predicted SOC stock maps are presented, taking into account three different SSP scenarios for MA and the AP. The SSI, including a: Low Island, b: Elephant Island, and c: the James Ross, Vega, Seymour, and Snow Hill Islands, are**

depicted at the centre of the left squares. The bar chart at the bottom illustrates the estimated SOC stocks categorized by island, considering the variations across different SSP scenarios.



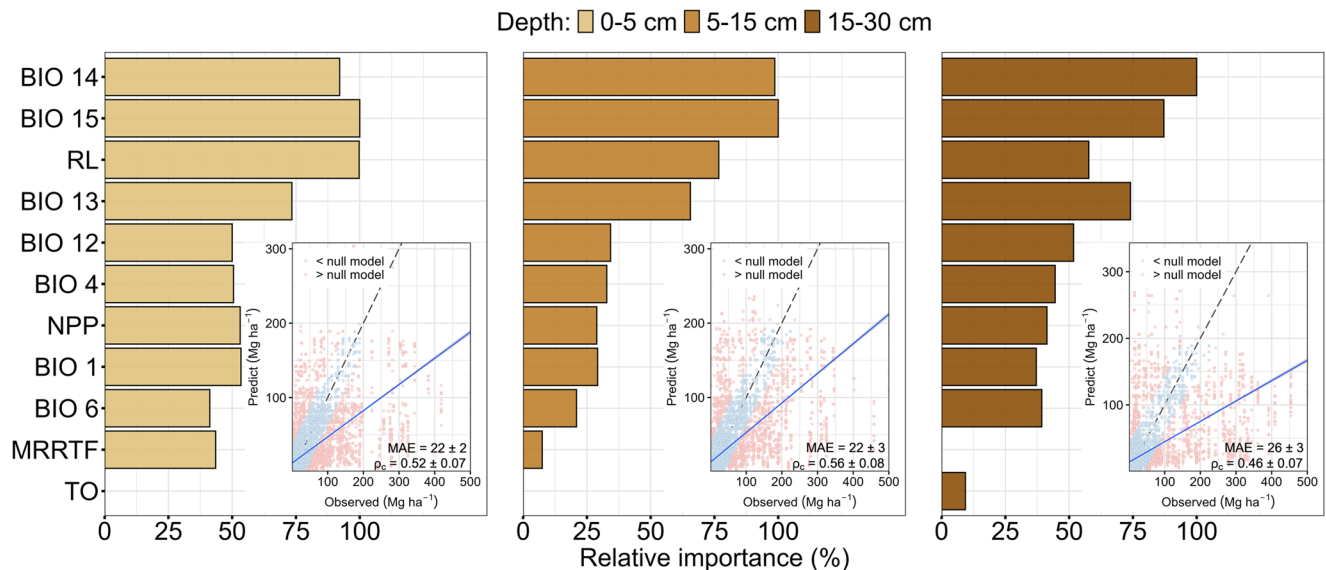


**Fig. 3 | Categorical importance of predictor variables for soil organic carbon stocks values as determined by the Random Forest algorithm.** An importance of variables analysis by the Random Forest algorithm, employing the listed variables, was used to discern the relative importance of environmental factors in predicting the responses of SOC stocks and content to warming. BIO 14: precipitation of the driest month; BIO 15: precipitation seasonality; RL: ridge level; BIO 13: precipitation of the wettest month; BIO 12: annual precipitation; BIO 4: temperature seasonality; NPP, net primary production; BIO 1: annual mean temperature; BIO 6: minimum

temperature of the coldest month; MRRTF: multi-resolution of ridge top flatness; TO: topographic openness. Insets display the performance of the Random Forest model, with metrics such as correlation coefficient and mean absolute error (MAE), along with determination coefficients. The blue line inside each square indicates the correlation between the values estimated and those observed by the model (Random Forest). The dotted line indicates the ideal correlation between what is estimated and what is observed.

depths (Fig. 3). In predicting SOC stocks, climatic environmental variables (BIO 1, 4, 10, 12, 13, 14, and 15), specifically temperature and precipitation conditions, emerged as the most crucial factors governing increase in SOC stock under all SSP warming scenarios and across all analysed soil depths. Our findings highlight not only the substantial correlations between precipitation and temperature that control SOC stocks in MA and AP, but also underscore the pivotal role of diverse climatic conditions in regulating SOC stock dynamics in response to climate change.

Our findings show that precipitation extremes, as indicated by variables BIO 14 and BIO 13, play a more crucial role in regulating SOC stocks in MA and AP than temperature variations (Fig. 3). This suggests that temperature increases have a less direct impact on SOC stocks compared to precipitation extremes. Nevertheless, temperature increases do affect precipitation patterns, and together, these climatic variables influence SOC stocks. Furthermore, while mean precipitation data (BIO 12) were also analysed, they proved less significant than the extreme precipitation data (BIO 14 and BIO 13) (Fig. 3). Our results reveal a strong correlation between SOC stocks and both precipitation and temperature. This indicates that the SSP climate change projections higher temperatures and precipitation in MA and AP will significantly enhance the carbon sequestration potential of ice-free areas and soils in the MA and AP region.

The variable ridge level (RL), which refers to the elevation of a ridge, explains 100% of the estimated SOC stocks within the surface layer. High RL indicates a proneness to erosion which significantly influences (0–5 cm depth, Fig. 3). Erosion significantly influences soil organic matter dynamics and plant community colonization, especially in periglacial-semiarid pedogeomorphic systems characterized by steep slopes<sup>26</sup>, as observed in our MA and AP study site. In regions experiencing periglacial erosion (freezing and thawing of water in soil pores and on slopes in cold environments, which cause specific types of erosion), continuous removal of surface materials, such as soil, organic carbon, and plant propagules, poses challenges for establishing vegetation and maintaining organic carbon<sup>27–29</sup>. Simultaneously, in such terrains, localized depositional landscape positions can serve as repositories for SOC stocks, as these areas experience lower erosion rates and provide more favourable conditions for the establishment of plant

communities<sup>30</sup>. This contributes to the overall preservation of SOC within the landscape. This intricate interplay between topography, erosion, and deposition highlights the nuanced nature of SOC stock distribution in environments marked by heterogeneous topography in MA and AP<sup>31</sup>. In addition, considerable portions of the high areas in MA and AP consist of flat terrains (plateaus, moraines, platforms)<sup>32</sup>, which are not subjected to intense erosive processes, but simultaneously have low levels of SOC due to more arid pedoclimate<sup>33</sup> and a decrease in vegetation abundance with increasing altitude<sup>34</sup>. Such high flat terrain areas experience lower temperatures, reduced humidity, and desiccating winds that not only decrease soil moisture but also hinder the establishment of vegetation.

Another notable environmental variable was NPP, mainly in the 0–5 cm soil layer, demonstrating an importance exceeding 50% in predicting SOC stocks (Fig. 3). In the context of warming scenarios, NPP tends to increase with progressive rises in temperature and humidity. Moreover, as temperatures and precipitation rise, glaciers tend to retreat, leading to an increase in ice-free areas. This could potentially result in the expansion of plant communities and an upsurge in NPP.

The comparison between estimated and observed values suggests that predicted SOC stock values may still be underestimated (Fig. 3). The actual values might be even higher, given that the predicted values fall below the ideal reference line (black) (Fig. 3). Although training data with actual samples were used to fit the SOC stocks prediction model, a tendency for overfitting was observed in the predictions, particularly in underestimating the estimated SOC stock values. The estimated SOC stock values range from 0 to 100 Mg ha<sup>-1</sup>. The highest and lowest SOC stock values correspond to greater prediction errors, whereas median SOC stock values are associated with smaller prediction errors (Fig. 3).

### Shifts in MA and AP SOC dynamics and soil-atmosphere-biosphere interaction patterns

Data in Figs. 4, 5 and 6, supplementary information illustrate, in details, how wetter-drier and hotter-colder conditions across MA and AP regions impact SOC stocks. The existence of a climate gradient, encompassing temperature and precipitation, linked to an NPP gradient affects estimated SOC stock

values. These environmental variables correlate with both latitude and longitude, with latitude exerting a more pronounced influence on temperature, and longitude on precipitation. Consequently, temperature and precipitation exhibit a declining climatic gradient from north to south, which also aligns with a decrease in the NPP gradient (Figs. 4, 5 and 6, supplementary information). However, the MA shows a more homogeneous pattern of precipitation and temperature due to the islands being relatively aligned longitudinally, which results in consistent patterns of NPP (Figs. 4, 5 and 6, supplementary information). There is a connection between these environmental variables and the current SOC stock values, evidenced also in the observed data. Notably, SOC stock values decrease in tandem with diminishing temperature, precipitation, and NPP.

The spatial dependence plots generated from our SOC stock predictive model suggest a robust and positive correlation of SOC stock with both the annual mean temperature and annual precipitation in Antarctica (BIO 1 and BIO 12). Similarly, the minimum temperature of the coldest month and the precipitation of the driest month (BIO 6 and BIO 14) show a strong positive correlation with SOC stocks (Fig. 4). A consistent pattern is observable in the SOC stock curves, indicating a tendency for values to increase at different depths. The positive relationship between SOC and BIO 1, BIO 12, BIO 6, and BIO 14 implies that future climate change predictions of increased temperature and precipitation could significantly enhance the potential of MA and AP soils in ice-free areas to function as carbon sinks. The validity of these findings is further supported when we analyse and cross-reference the information with the partial dependence of SOC stocks on NPP (Fig. 4). Our results suggest a relationship between SOC stock values and increase in NPP, which is in turn associated with rises in temperature and precipitation, as indicated by the variables BIO 6, BIO 14, BIO 1, and BIO 12 (Fig. 4).

The projections from the three distinct SSP scenarios directly influenced our predictive SOC stock model (Fig. 4). These projections indicate a estimated increase in precipitation and mean temperature in MA and AP coupled with a rise in extreme climate events. Consequently, there will be a projected increase in ice-free areas, which could facilitate plant community colonization and, ultimately, an increase in NPP and soil carbon input.

### Success of the SOC predictive model and different SOC sources in Maritime and Peninsular Antarctica

The dynamics of SOC in both MA and AP regions are shaped by a complex interplay of biological and environmental factors<sup>8,11</sup>. In soils where seabird colonies are present in some specific areas of Maritime Antarctic soils, SOC is largely influenced by microbial contributions and stabilized humified organic carbon, with key processes including soil guano phosphatization (in penguin rookery)<sup>4,35</sup>. Soil temperature and moisture variability play a crucial role in SOC dynamics as indicated by BIO1, BIO6, BIO12, BIO13, and BIO14 (Fig. 4). Thomazini and Mendonça<sup>6,36,37</sup>, highlighted the link between CO<sub>2</sub> emissions and soil temperature and moisture in Antarctica, especially near the 0 °C isotherm, with temperature driving carbon mineralization. In contrast, Eastern Antarctic soils derive SOC from a variety of sources, including resilient microorganisms like cyanobacteria, blue-green algae, and fungi, which are instrumental in organic matter production and decomposition<sup>8</sup>. Lichens and mosses also play a vital role despite their slow decomposition rates<sup>11</sup>. Furthermore, native vascular plants like *Deschampsia antarctica* and *Colobanthus quitensis* contribute through their residues<sup>38</sup>, while air currents transport additional organic material from distant regions. It is important to note that invasive plants, such as *Poa annua*, also may contribute to significant SOC inputs, especially in the context of climate change<sup>39</sup> and newly exposed areas after glaciers retreat<sup>40</sup>. However, studies examining the relationship between SOC inputs and invasive plants in Antarctica remain scarce. Understanding these varied contributions is essential for a comprehensive view of carbon dynamics in Antarctic soils, as the effects of glacier retreat vary among plant species<sup>41</sup>. Although all these SOC sources are well known, we do not consider all of them simultaneously in our model for two reasons: 1) not all sources of SOC

as predictor variable are spatially explicit at the studied site, and 2) we apply the principle of parsimony in modeling SOC stocks, where the explanation of the phenomenon is provided by the simplest model with the fewest predictor variables. In addition, predictive models indicate a potential increase in NPP; however, Antarctica's geographical isolation poses a significant obstacle. Although it has recently been recognized that invasive species are colonizing parts of Antarctica following glacier retreat and altering certain soil characteristics<sup>40,42</sup>, they cannot yet be incorporated into models due to the limited availability of reliable future data.

There was variation in the model's performance in predicting the spatial distribution of SOC stocks across different soil depths. Concordance correlation coefficient index ( $\rho_c$ ) considers that the model indicated the best performance for the 5–15 cm layer (0.56), followed by the surface layer 0–5 cm (0.52), and the 15–30 cm layer (0.46) (Fig. 5). In addition, errors in the prediction of SOC stocks, measured by the mean absolute error (MAE) and root mean square error (RMSE) parameters, increased with depth (Fig. 5). Specifically, the error values (MAE) for the 0–5 cm, 5–15 cm, and 15–30 cm soil layers were 37.24, 39.62, and 42.92, respectively, while the RMSE values were 58.37, 61.51, and 69.53, respectively (Fig. 5). Meanwhile, the values of uncertainty in the prediction of the SOC stocks were 58.37, 61.51, and 69.53 for the 0–5 cm, 5–15 cm, and 15–30 cm layers, respectively, with the highest  $\rho_c$  values and the lowest MAE and RMSE values (Fig. 5). When assessing the deviation of errors in our model in comparison to the null model, we observe a superior performance in the fit of our model. Notably, when examining the MAE, this difference is more pronounced than in the RMSE. The RMSE, being an error metric highly sensitive to extreme values (outliers), accentuates this behaviour, particularly in the context of soil carbon stocks in MA and AP. This sensitivity implies that the model demonstrates lower accuracy in predicting extreme SOC stock values, as evidenced by its inferior performance within these ranges (Fig. 5). This is justified because RMSE evaluates the effects of outliers, considering extreme values in the prediction. Additionally, this suggests that the model exhibits lower accuracy in predicting samples with extreme values of SOC stocks, as indicated by the lower performance associated with these instances.

### Limitations and uncertainties

The space-for-time modelling approach employed in assessing SOC stocks is subject to some key limitations and uncertainties. Initially, the model did not consider the evaluation of the impacts stemming from additional global change factors concomitant with warming, such as elevated carbon dioxide (CO<sub>2</sub>) levels and nitrogen deposition. Given the generally positive influences of heightened CO<sub>2</sub> and nitrogen deposition on plant growth<sup>43,44</sup>, our model could have potentially underestimate SOC stocks. Another limitation concerns the representation of physico-chemical attributes of soil that are related to SOC. By incorporating the soil's physico-chemical attributes, our model could attain enhanced performance and accuracy in predicting SOC stocks. While our database stands as the one of the largest global Antarctic soil databases<sup>16</sup>, these data are not spatially continuous across the MA and AP region. Additionally, detailed data on soil types (Orders) were not specifically incorporated into our model. This limitation arose because, similar physico-chemical information, soil type information was not available in a spatially continuous manner.

Another limitation is that the modelling approach makes an implicit assumption that the latest changes in the environmental conditions of the ice-free areas (last two decades), soils, and regional warmth was similar or affected the response of SOC stocks to warming in a similar manner, which may not be true. More robust analyses at regional scales would be necessary to assess these effects; however, there exists a deficiency in detailed data on regional environmental conditions for the areas evaluated in this study. Furthermore, our model does not account for the dynamics of glacier retreat, the volume and distribution of meltwater in the face of increased precipitation, and the size of the ice-free areas. To enhance the accuracy and performance of the models, it is imperative to further elucidate the cold landscape dynamics and their relationship with other

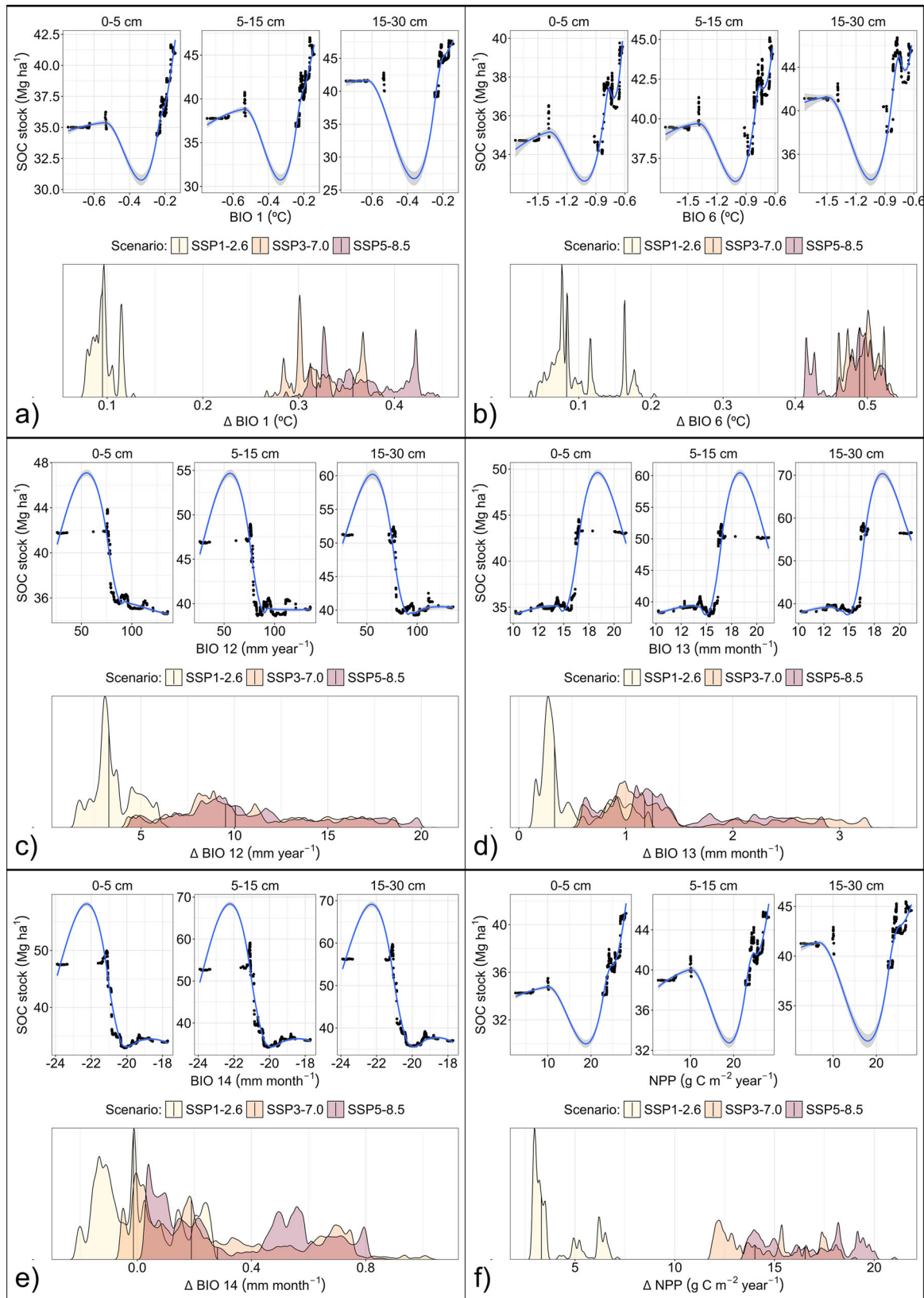


**Fig. 4 | The relationship between climatic variables and predicted s soil organic carbon stocks values.** The relationship between climatic variables and estimated SOC stock values is explored in consideration of various SSP scenarios and across different soil depths in the ice-free areas of Maritime and Peninsular Antarctic. **a** and **b** explore the relationship between mean annual climatic variables, specifically annual mean temperature and annual precipitation in Antarctica (BIO 1 and BIO

12), and the predicted SOC stock. **c**, **d**, and **e** investigate the relationship between extreme climatic events, specifically the minimum temperature of the coldest month, precipitation of the wettest month, and the precipitation of the driest month (BIO 12, BIO 13, and BIO 14), and the estimated SOC stock. **f** examines the relationship between NPP and estimated SOC stock values.

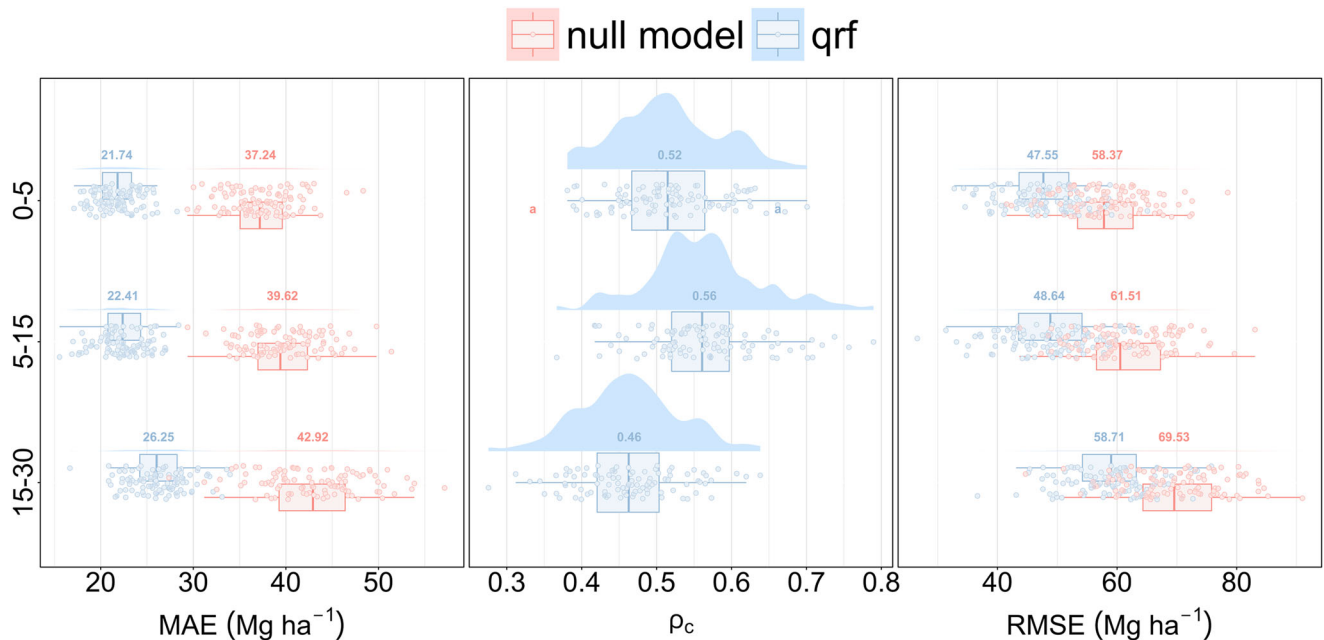


**Fig. 5 | Performance metrics for predicting soil organic carbon stock content.** The performance parameters of the model in predicting SOC stocks using the Quartile Random Forest (qrf), including mean absolute error (MAE), concordance correlation coefficient ( $\rho_c$ ), and root mean squared error (RMSE).

environmental variables. Nevertheless, the incorporation of these variables into the models is intricate, and there is a dearth of studies that elucidate this dynamic.

Plant biomass inputs in surface soils play a crucial role in changes to SOC stock. As glaciers retreat, they expose new areas for plant colonization, while warmer temperatures enhance the plants' growth<sup>45</sup>. However, extreme heat can also have negative effects on plant growth. Cavieres et al. (2016)<sup>46</sup> demonstrated that leaf temperatures exceeding 20 °C can impair photosynthesis, reducing plants' ability to tolerate freezing temperatures, which is a critical trait for colonizing harsh environment, such as those formed by glacier retreat. The glacier retreat and plant colonization leads to rapid soil development, with increased vegetation cover correlating with higher levels of SOC, nitrogen, and organic matter in the soil<sup>47</sup>. However, it is important to note that the areas currently colonized by vascular plants in MA and AP are limited to a few locations in ice-free areas<sup>48</sup>. For new areas in MA and AP to be colonized due to increased temperature and nutrient availability, facilitating SOC transport and stock, plant propagules must reach these areas. This limitation in our model arises from the absence of data on plant propagules and vegetative propagation trends, preventing their inclusion in future scenarios. Furthermore, a simple increase in NPP does not necessarily mean that new ice-free areas will be colonized by plant communities and, as a result, see increase in SOC stocks. Temperature increase could lead to extreme climate conditions as colder and harsher winters, potentially resulting in reduced snowmelt and increased aridity in some areas<sup>49</sup>. This could restrict plant colonization and can result in browning of the landscape. Therefore, it remains unclear whether vegetation in MA and AP will expand (and greening) in response to warming or if increased evaporation will cause dieback of highly adapted organisms (browning)<sup>49,50</sup>. Additionally, it was not possible to include these factors as predictor variables in our model for SOC stock.

SOC stock levels and NPP are also influenced by the biological activity of regional fauna, particularly penguins in areas where *Pygoscelis* species are present, as their excrement significantly contributes to the organic matter<sup>4,38</sup>. The behavior of fauna in MA and AP has been impacted by global warming, leading to rapid demographic changes in some penguin populations and affected areas<sup>51,52</sup>. However, incorporating animal behavior data into our model was not feasible, as there is no sufficiently detailed fauna behavior database at the regional level, nor future projections considering SSP periods. This is another limitation of our study.

Despite its limitations, this study furnishes on-site evidence of robust negative carbon-climate feedback in the MA and PA soils (processes that reduce atmospheric CO<sub>2</sub> levels, helping to mitigate climate change effects), estimating minimum carbon sequestration values of 17.22, 24.58, and 23.54  $\text{Mg ha}^{-1}$  in the top 30 cm of soil under the warming scenarios of 1.5 °C, 2.5 °C, and 4 °C, respectively (Fig. 2). Notably, proglacial, periglacial, and paraglacial MA and AP systems are positioned to play a significant role in mitigating climate change by effectively reducing atmospheric CO<sub>2</sub> under global warming scenarios. Acknowledging the potential for carbon sequestration revealed in this research is crucial for offsetting carbon emissions from other global sources, thereby contributing to global warming mitigation efforts. In essence, our methodology relies on the most reliable information accessible and mitigates uncertainties through the assessment of variability within the produced ensembles. Offering insights into these uncertainty sources and the capacity to address them in forthcoming estimations is essential for a more thorough evaluation of data uncertainty.

## Discussion

Our results revealed that most of the MA and AP soils in ice-free areas may be a sink of carbon considering future climate change and global warming scenarios, implying a negative feedback mechanism for atmospheric CO<sub>2</sub>. Notably, the findings also illustrate that some MA and AP regions presently characterized by higher SOC stocks are inclined to experience carbon losses in response to global warming, elevated temperatures, and increased precipitation (except Nelson, Hope Bay, Half Moon, and Ardley) (Fig. 2). Conversely, areas with lower SOC stocks tend to accumulate more carbon under these conditions. Our findings suggest that atmospheric carbon feedback dynamics in certain regions of MA and AP tend toward negative feedback, as the ice-free areas and Cryosols in these regions have lower SOC stocks<sup>4,53</sup>.

The size of ice-free areas and pedogenetic factors also influence SOC stocks. In the Antarctic ice-free area (49,500 km<sup>2</sup>) has an estimated SOC level of 0.725 Pg C in its soils<sup>4</sup>. Cryopedogenic processes in Antarctica like cryoturbation, in frozen conditions, hinder decomposition, leading to prolonged sequestration of SOC in permafrost-affected soils over millennia. The low temperatures result in less molecularly complex organic matter, making a portion of the stored carbon susceptible to mineralization upon



permafrost thawing<sup>54</sup>. However, it was not possible to evaluate this dynamic in our model. In addition, SOC stocks are dependent on soil depth. SOC stocks in deeper layers show a general tendency to store less SOC (Fig. 1, supplementary information). The observed phenomenon may be ascribed to the diminished root biomass and reduced availability of high-quality carbon substrates, leading to a small amount of SOC decomposition in deeper soil depths<sup>55</sup>, particularly in areas where cryoturbation processes are absent.

The atmospheric carbon sink effect on MA and AP soils was most pronounced in the upper soil layers, decreasing with depth (Fig. 1, supplementary information). Climatic factors governing the increase in SOC stocks in surface layers primarily involve changes in temperature and precipitation, encompassing both elevations in the averages and extremes of climatic events. Additionally, our predictive model suggest an increase in NPP in newly exposed areas due to the likely colonization and/or expansion of plant communities in AP and MA. The increase in NPP, driven by rising temperatures and precipitation and newly exposed areas as indicated by our model, has significant potential to enhance carbon sequestration through processes such as photosynthesis<sup>36</sup>, increased biomass production, and greater carbon storage in the soil due to increase in SOC stocks. As a result, our mathematical model suggest a scenario in which carbon inputs from plant biomass exceed the rates of carbon release due to increased decomposition, which is further exacerbated by the rises in temperature and precipitation in the cryosphere associated with global warming, as outlined by the IPCC<sup>56,57</sup>.

The substantial pedoenvironmental diversity (landscape variability, including factors such as climate, lithology, topography, and soil attributes) led to the observation of significant outliers in SOC values estimated by our model. Furthermore, some of the soil samples used as input data in our predictive SOC stock models were collected from penguin rookeries in MA and AP. These soils are formed by substantial guano inputs from penguins and seabirds, making them significant factors influencing SOC dynamics<sup>58</sup> and resulting in higher SOC stock values in certain samples. However, despite the high SOC levels in these areas, their size is relatively small and unrepresentative at the Antarctic scale. Soil depth and lithology play pivotal roles in this context. Some of our soil samples used as input data in our predictive models were collected from shallow soils on basaltic and andesitic substrates, identified as the most responsive sites for CO<sub>2</sub> emissions. In contrast, other samples came from deeper soils affected by sulphides in pyritized materials, which exhibited different behaviours, as highlighted by Pires<sup>59</sup>. Additionally, the elevated stoniness observed in shallow soils contributed to a reduction in SOC stocks.

Our results indicated that for soils in ice-free areas of MA and AP, the main environmental factors controlling the variability of SOC stock under different climate change scenarios are temperature, precipitation, and net primary production. This is consistent with the findings of Gautam (2022)<sup>60</sup>, who assessed the vulnerability of soils in the Continental United States to climate-induced SOC loss by 2100. Furthermore, as noted by Gautam (2022), soil attributes such as soil type and its characteristics also play a role in determining SOC stock. Although we do not have spatially continuous data on soil types, we ensured environmental variability by collecting samples from different pedoenvironments, landscape positions, various lithologies, and distinct climatic conditions in paraglacial, periglacial and proglacial environments. Important and innovative studies conducted by Wang (2022) and Wang (2023)<sup>61,62</sup> demonstrated that global soils tend to be a source of carbon to the atmosphere under global warming scenarios (positive carbon feedbacks). However, our results revealed that, in most areas of MA and AP, soils are likely to act as a CO<sub>2</sub> sink under global warming scenarios. It is important to highlight that, in MA and AP, some islands may act as CO<sub>2</sub> sources, while a few others may show neutral SOC responses under different climate change scenarios, following the same tendencies demonstrated by Wang (2023)<sup>62</sup> which revealed distinct (positive, neutral, or negative) SOC responses in global soils under global warming. In addition, our findings also align with the authors' conclusions that the largest sinks tend to occur in cold-desert environments with

minimal vegetation, and that the most significant SOC sink effects in MA and AP soils are likely to occur in the most superficial soil layers, as observed by Wang (2022)<sup>61</sup>.

The estimation of SOC in ice-free areas of MA and AP represents a pioneering effort, employing quantitative-qualitative modelling to incorporate key variables influencing SOC stocks. When considering the storage of SOC, a critical soil attribute is the soil texture, mainly the fine particle fraction, comprising clay and silt. The majority of soils sampled and incorporated into our model (Method section) exhibit approximately 10% clay and 40% silt<sup>63,64</sup>, with the coarse fraction (sandy loam texture) being predominant<sup>23</sup>. The fine texture of the soil plays a pivotal role in determining the capacity for microaggregate formation and the creation of protected pools essential for storing organic carbon. The contribution of fine particles in soil to carbon storage in these pools is facilitated by their extensive surface area for organic carbon adsorption and the formation of smaller microaggregates in the silt size range<sup>65,66</sup>.

## Conclusion

Our study reveals that the largest and wettest ice-free areas of MA and the AP have the potential to function as a reservoir of SOC. Across the three SSP scenarios, the estimated percentage increments in SOC stocks are 27.67% for SSP1-2.6, 53.34% for SSP3-7.0, and 52.89% for SSP5-8.5. SOC stocks are projected to increase significantly (from 359 ± 146 Mg to 686 ± 197 Mg), primarily within the initial 0–15 cm of the soil layer. This enhancement is attributed to negative feedback loops intertwined with soil carbon storage and climate warming, which are evident across all topsoil layers and scenarios of global warming outlined in the SSP scenarios. The key environmental variables crucial in predicting SOC stocks included those associated with net primary production, temperature, and precipitation. Ice-free areas that naturally exhibit lower SOC stock values are typically estimated to see an increase in SOC stocks (the majority of areas), whereas those with higher values are estimated to see a decrease in SOC stocks. Our results demonstrated that increases in SOC values tend to follow a climatic gradient, correlating with rises in temperature and precipitation, which subsequently drive increases in NPP and newly exposed ice-free areas. Our model, employed for spatial prediction and modelling uncertainty in predicting SOC stocks, demonstrated satisfactory performance considering concordance correlation index.

## Methods

The investigation zone encompassed MA and the AP (Fig. 3, supplementary information). The detailed study area, encompassing all islands, locations, and ice-free areas are presented in Table 2 (supplementary information). The climatic and vegetative characteristics of ice-free regions exhibited significant variations based on their geographical coordinates, encompassing both latitude and longitude. Within the South Shetland Islands (SSI) in MA, there is the occurrence of a sub-Antarctic moist and mild maritime climate. The mean annual precipitation ranges from 350 to 800 mm, coupled with a mean annual air temperature averaging around −2 °C<sup>67</sup>. Antarctic moss carpets proliferate in regions with increased water availability, whereas lichens dominate the arid highlands<sup>27</sup>. The flora includes two vascular plant species, *Deschampsia antarctica*, *Colobanthus quitensis*, and macroalgae communities<sup>68</sup>. In the AP, the climate leans towards aridity, with Hope Bay experiencing a mean annual temperature of −5 °C and JRI at −6 °C<sup>69</sup>. The mean annual precipitation in this region spans from 300 to 500 mm<sup>67,69–71</sup>. The altitude in MA ranges from 0 to 400 meters, whereas in the AP it varies from 0 to 600 meters.

The lithology of the area is diverse, primarily comprising igneous, metamorphic, and sedimentary rocks, along with marine terraces containing undifferentiated sediments. The predominant rock types constituting the islands of MA and the AP include marine sandstones, mudstones, basalt, basalt-andesite, pyritized-tuffites, diorites, olivine-basaltic, and andesite-basaltic, as well as andesitic lavas associated with tuffs, basaltic lavas, tuffs, conglomerates, and drifts<sup>23,72–77</sup>. The geomorphology of the ice-free areas is characterized by a variety of erosive and depositional

landforms, reflecting the complexity of geomorphic processes<sup>32</sup>, different altitudes, and landforms.

Pedologically, the soils found in the AP and MA are not well-developed, composed mainly by Leptosols, Regosols, Fluvisols, Cambisols, and Cryosols, many with Gelic properties according to the Base for Soil Resources (World Reference Base for Soil Resources)<sup>23,78,79</sup>. The physical and chemical attributes of these soils exhibit variation, with some being influenced by processes such as phosphatization (on penguin rookeries), salinization, and sulphurization associated with sulphide materials.

### Soil data and bulk density analyses

Legacy soil physico-chemical data, primarily generated by the Brazilian Terrantar Group through extensive soil surveys conducted in the past two decades (Table 2, supplementary information) during austral summer in MA and the AP, were employed to predict SOC stocks. This dataset includes comprehensive soil profiles comprising both the surface and subsurface, varying from 0–30 cm, and was collected across the primary ice-free regions. After initially filtering, we utilized data on SOC content and soil bulk density, creating a dataset containing 2802 observation samples with information on SOC content, soil depths, and associated geographic coordinates. The relatively low number of samples from the MA and AP regions underscores the necessity for re-evaluating large-scale estimates of SOC stocks. Certain points merit consideration. First, the soil samples in this study originate from various heterogeneous areas and were collected for diverse purposes using distinct methodologies. Employing a standardized protocol within a common experimental design through a specific survey would likely enhance SOC stock estimates by minimizing undesired variability among samples. Second, enhancing the precision and spatial resolution of the underlying data layers would instill greater confidence in stock distribution and local-level estimates. Lastly, acknowledging the dynamic nature of stocks influenced by periglacial, paraglacial, and glacial processes is crucial. Although incorporating temporal and historical factors poses challenges in large-scale Antarctic studies, these factors contribute significantly to the variance in SOC stocks beyond the explanatory capacity of our model.

The soil bulk density was analysed in an initial database comprised 127 samples. The soil bulk density was determined using the graduated cylinder method<sup>80</sup>. This method involves obtaining the mass of the soil sample by weighing it after compacting it in a test cylinder to a pre-determined volume. The subsequent density calculation takes into account a humidity correction factor. This method is suitable for Antarctic soil conditions, which are characterized by sandy-silt texture and high stoniness, as other methods for determining soil bulk density are not feasible during sample collection.

### Spatial prediction and uncertainty quantification of Antarctic SOC stocks

We created a regression method, a pedotransfer function for soil bulk density<sup>81</sup> based on an initial database comprising 127 soil bulk density samples, utilizing easily obtainable field variables related to soil bulk density as predictors<sup>82</sup>: pH, soil organic carbon, sand, silt, and clay content (Table 2, supplementary information). It is important to emphasize that the modelling of SOC stocks for both present and future scenarios did not incorporate the physico-chemical attributes of the soils. Two primary reasons account for this: 1) the unavailability of spatialized data for several attributes and 2) the absence of such data for future scenarios. To determine the optimal fit for the pedotransfer function, we employed four machine learning algorithms and utilized the nested leave-one-out cross-validation method (nested-LOOCV) described in detail by Mello<sup>83,84</sup>. The nested-LOOCV method involves a double-loop process, comprising an inner loop for hyperparameter adjustment and an outer loop for determining model performance. In the initial loop, the model is trained using a dataset of size  $n - 1$ , and the testing is conducted in the subsequent loop with the omitted sample<sup>83</sup>. This omitted sample is then utilized to validate both the test and training performance. The chosen model was the Random Forest (RF),

showcasing the optimal performance when evaluating parameters such as  $\rho_c$  with a value of 0.44, MAE at  $0.13 \text{ g cm}^{-3}$ , and RMSE with a value of  $0.18 \text{ g cm}^{-3}$ . For each of the 2675 soil samples lacking density data, 127 predictions of soil bulk density values were generated (following the nested-LOOCV), and the average of these 127 predictions (Table 2, supplementary information) was utilized for each respective sample. Following this, SOC stocks were computed using Eq. 1.

$$\text{SOC stock} = \frac{\text{SOC} \times \text{BD} \times e}{10} \quad (1)$$

where:

SOC stock represents the stock of soil organic carbon in  $\text{Mg ha}^{-1}$ ,

SOC is the soil organic carbon content in  $\text{g kg}^{-1}$ ,

BD is the bulk density of the soil in  $\text{g cm}^{-3}$ , and

$e$  is the thickness of the soil layer in cm.

We chose to use concordance correlation coefficient ( $\rho_c$ ) instead of coefficient of determination ( $R^2$ ) due to its greater robustness in assessing the agreement between predicted and observed values, especially in situations where it is essential to consider systematic bias in the data<sup>85</sup>. Unlike  $R^2$ ,  $\rho_c$  accounts for both precision (correlation) and accuracy (proximity to the 45-degree line), whereas  $R^2$  is limited to evaluating the precision in explaining data variability. Since our objective is to develop models that quantify soil organic carbon stocks in Antarctica with high accuracy,  $\rho_c$  proves to be more appropriate.

We standardized SOC stocks at depths of 0–5 cm, 5–15 cm, and 15–30 cm following the Poggio method<sup>24</sup>. This harmonization was achieved using splines, implemented with the “spline” function from the “mpspline2” package<sup>86</sup> in the R programming language. To visually represent the SOC stocks in different soil layers/depths, we conducted an analysis using R software version 4.3.2, employing the ‘aqp’ package from the Algorithms for Quantitative Pedology<sup>87</sup>. This package facilitated the organization of a cohesive set of SOC stock data, providing qualitative SOC stock visualization, aggregation, and classification in soil profiles. We organized an environmental predictor explanatory database that included eight bioclimatic variables (BIO 1 = annual mean temperature; BIO 4 = temperature seasonality (standard deviation  $\times 100$ ); BIO 5 = maximum temperature of the warmest month; BIO 6 = minimum temperature of the coldest month; BIO 12 = annual precipitation; BIO 13 = precipitation of the wettest month; BIO 14 = precipitation of the driest month; and BIO 15 = precipitation seasonality), vegetation (NPP), and relief (a digital elevation model and other derived morphometric variables) (Table 3, supplementary information). Recognizing the relatively stable nature of relief over decades, we treated it as a static variable in our model. Consequently, we maintained identical relief information for both the present (historical data from 1981 to 2010) and the future (2081–2100), while considering climatic and vegetation variables as dynamic.

The digital elevation model with an 8-meter resolution was obtained from the Reference Elevation Model of Antarctica (REMA)<sup>88</sup>, and the 52 morphometric variables were derived using the RSAGA package<sup>89</sup>. Historical and future climate and vegetation variables were sourced from Chelsa v 2.1.1<sup>90</sup>. Chelsa provides variables with a spatial resolution of 1 km for various periods, climate models, and SSPs from the IPCC. We selected the present period with historical data (1981–2010) and the latest available projected future period (2071–2100). For the future climate models, we utilized five available models (GFDL-ESM4, IPSL-CM6A-LR, MPI-ESM1-2-HR, MRI-ESM2-0, and UKESM1-0-LL), each characterized by distinct climate sensitivity balances<sup>91</sup>. Regarding scenarios, we incorporated three contrasting SSP scenarios developed by the IPCC to explore different plausible futures for the world based on various socioeconomic factors and climate policies: SSP1-2.6 (pathway to global sustainability: effective mitigation and balanced growth, aligned with the ambition of limiting global warming to  $1.5^\circ\text{C}$ ), SSP3-7.0 (persistence of inequality: uneven growth and emerging climate challenges, aligned with the ambition of limiting global warming to  $2.5^\circ\text{C}$ ), and SSP5-8.5 (prioritized development: high emissions

and extreme climate risks, aligned with the ambition of limiting global warming to 4 °C<sup>92</sup>. All variables were harmonized to a spatial resolution of 8 meters (using the same resolution of digital elevation) and projected into the South Pole Stereographic system (ESRI:102021) using the “terra” package<sup>93</sup>.

We employed the quantile random forest (qrf) model, as proposed by Meinshausen<sup>94</sup>, which was implemented in the “caret” package developed by Kuhn<sup>95</sup> within the R environment<sup>96</sup>. This model offers distinct advantages compared to alternative algorithms, as it allows for the quantification of both quantiles and the standard deviation of predicted values. Initially, we executed two sequential processes to filter the explanatory predictors. The first process involved assessing correlation, wherein we removed one variable from pairs exhibiting a Spearman correlation greater than  $|0.95|$ . Subsequently, the remaining variables underwent selection based on importance. This involved subjecting them to the interactive backward recursive feature elimination algorithm, facilitated by the “caret” package. We systematically tested subsets of variables, ranging from 2 to the total number of variables, incrementally adding one variable at a time and assessing performance. Finally, we identified the subset demonstrating the best performance, discarding variables that contributed minimally to the model.

Once the subset of variables was selected, we fine-tuned the qrf model using cross-validation with 10 replications and hyperparameter optimization (*tuneLength* = 10). In response to concerns about cross-validation potentially yielding performance metrics that do not align with the model's generalizability, we introduced a repeated testing structure. We divided the training set into cross-validation (80%) and external testing (20%) subsets. We selected the optimal variables for the training set, fine-tuned the model with optimized hyperparameters, and assessed performance using the test set. This process was repeated 100 times, each time with different training and testing arrangements generated using the “createDataPartition” function from the *caret* package. Consequently, this approach yielded diverse results for both the subset of variables and the associated performance values.

Additionally, we computed a null model to serve as a benchmark for comparison with our model and to assess its viability. The model, adjusted for present and future predictions, was calibrated using all SOC stock data. For the predictions, we estimated the median (Q50), uncertainties, quantiles 0.25 and 0.75 (Q05, Q75), and the coefficient of variation. Maps were generated for both present and future scenarios across three SSP scenarios, five climate models, and three soil depths, maintaining a spatial resolution of 8 m. To gauge the importance of variables, we conducted analyses using relative importance through permutation and partial dependence techniques. The entire modelling process and figure creation were carried out within the R environment (R Core Team, 2023), with primary support from the *mdsFuns* package<sup>97</sup>, *labgeo* package, and *caret* package<sup>95</sup>.

The map layouts were created using ArcGIS Pro version 3.0 software. SOC stock values were categorized into ranges with upper and lower limits to form four distinct classes. Each class encompassed 25% of the data, and this classification was achieved using the *quantile* function within ArcGIS.

## Data availability

The datasets used in this study are publicly available on GitHub at [https://github.com/moquedace/soc\\_stock\\_antarctica](https://github.com/moquedace/soc_stock_antarctica). The study results, including model outputs and predicted rasters for present and future soil organic carbon stocks, are archived on Zenodo and can be accessed via <https://doi.org/10.5281/zenodo.14004139>.

## Code availability

The R codes and datasets used in the research are available in a GitHub repository under the [https://github.com/moquedace/soc\\_stock\\_antarctica](https://github.com/moquedace/soc_stock_antarctica). The results, along with maps for all depths, are accessible on Zenodo via the <https://doi.org/10.5281/zenodo.14004139>.

Received: 1 May 2024; Accepted: 28 November 2024;

Published online: 24 February 2025

## References

1. Turner, J. et al. The instrumental period. *Antarct. Clim. Chang. Environ. Sci. Comm. Antarct. Res. Cambridge* 183–298 (2009).
2. Vaughan, D. G. et al. Recent rapid regional climate warming on the Antarctic Peninsula. *Clim. Change* **60**, 243–274 (2003).
3. Gray, A. et al. Remote sensing reveals Antarctic green snow algae as important terrestrial carbon sink. *Nat. Commun.* **11**, 2527 (2020).
4. Bockheim, J. G. & Haus, N. W. Distribution of organic carbon in the soils of Antarctica. *Soil Carbon* 373–380 (2014).
5. Thomazini, A. et al. The current response of soil thermal regime and carbon exchange of a paraglacial coastal land system in maritime Antarctica. *L. Degrad. Dev.* **31**, 655–666 (2020).
6. Thomazini, A. et al. Spatial variability of CO<sub>2</sub> emissions from newly exposed paraglacial soils at a glacier retreat zone on King George Island, Maritime Antarctica. *Permafrost. Periglac. Process.* **25**, 233–242 (2014).
7. Schuur, E. A. G. et al. Permafrost and climate change: carbon cycle feedbacks from the warming Arctic. *Annu. Rev. Environ. Resour.* **47**, 343–371 (2022).
8. Gajanananda, K. Soil organic carbon and microbial activity: east Antarctica. *Eur. J. Soil Sci* **58**, 704–713 (2007).
9. Newsham, K. K., Garnett, M. H., Robinson, C. H. & Cox, F. Discrete taxa of saprotrophic fungi respire different ages of carbon from Antarctic soils. *Sci. Rep.* **8**, 7866 (2018).
10. Smith, H. J. et al. Microbial formation of labile organic carbon in Antarctic glacial environments. *Nat. Geosci.* **10**, 356–359 (2017).
11. Benavent-González, A. et al. Identity of plant, lichen and moss species connects with microbial abundance and soil functioning in maritime Antarctica. *Plant Soil* **429**, 35–52 (2018).
12. Bragazza, L. et al. Soil microbial community structure and enzymatic activity along a plant cover gradient in Victoria Land (continental Antarctica). *Geoderma* **353**, 144–151 (2019).
13. Roberts, P., Newsham, K. K., Bardgett, R. D., Farrar, J. F. & Jones, D. L. Vegetation cover regulates the quantity, quality and temporal dynamics of dissolved organic carbon and nitrogen in Antarctic soils. *Polar Biol* **32**, 999–1008 (2009).
14. Elberling, B. et al. Distribution and dynamics of soil organic matter in an Antarctic dry valley. *Soil Biol. Biochem.* **38**, 3095–3106 (2006).
15. Fisher, M. The Challenges of Doing Soils Research in Antarctica: A Day in the Life of Ed Gregorich. *Soil Horizons* **55**, 1–3 (2014).
16. Siqueira, R. G. et al. Modelling and prediction of major soil chemical properties with Random Forest: Machine learning as tool to understand soil-environment relationships in Antarctica. *CATENA* **235**, 107677 (2024).
17. Gomes, L. C. et al. Modelling and mapping soil organic carbon stocks in Brazil. *Geoderma* **340**, 337–350 (2019).
18. Wu, T. et al. Storage, patterns, and environmental controls of soil organic carbon stocks in the permafrost regions of the Northern Hemisphere. *Sci. Total Environ.* **828**, 154464 (2022).
19. Mishra, U. et al. Spatial heterogeneity and environmental predictors of permafrost region soil organic carbon stocks. *Sci. Adv.* **7**, eaaz5236 (2021).
20. Mishra, U., Gautam, S., Riley, W. J. & Hoffman, F. M. Ensemble machine learning approach improves predicted spatial variation of surface soil organic carbon stocks in data-limited northern circumpolar region. *Front. big Data* **3**, 528441 (2020).
21. Miner, K. R. et al. Permafrost carbon emissions in a changing Arctic. *Nat. Rev. Earth Environ.* **3**, 55–67 (2022).
22. Kåresdotter, E., Destouni, G., Ghajarnia, N., Hugelius, G. & Kalantari, Z. Mapping the vulnerability of Arctic wetlands to global warming. *Earth's Futur.* **9**, e2020EF001858 (2021).
23. Siqueira, R. G., Moquedace, C. M., Francelino, M. R., Schaefer, C. E. G. R. & Fernandes-Filho, E. I. Machine learning applied for Antarctic



- soil mapping: Spatial prediction of soil texture for Maritime Antarctica and Northern Antarctic Peninsula. *Geoderma* **432**, 116405 (2023).
24. Poggio, L. et al. SoilGrids 2.0: producing soil information for the globe with quantified spatial uncertainty. *Soil* **7**, 217–240 (2021).
25. Shi, Z. et al. The age distribution of global soil carbon inferred from radiocarbon measurements. *Nat. Geosci.* **13**, 555–559 (2020).
26. Musso, A., Ketterer, M. E., Greinwald, K., Geitner, C. & Egli, M. Rapid decrease of soil erosion rates with soil formation and vegetation development in periglacial areas. *Earth Surf. Process. Landforms* **45**, 2824–2839 (2020).
27. Ferrari, F. R. et al. Coupled soil-vegetation changes along a topographic gradient on King George Island, maritime Antarctica. *Catena* **198**, 105038 (2021).
28. García-Fayos, P., García-Ventoso, B. & Cerdà, A. Limitations to plant establishment on eroded slopes in southeastern Spain. *J. Veg. Sci.* **11**, 77–86 (2000).
29. Walker, D. A. et al. Calcium-rich tundra, wildlife, and the “Mammoth Steppe”. *Quat. Sci. Rev.* **20**, 149–163 (2001).
30. Walker, D. A. et al. Terrain, vegetation and landscape evolution of the R4D research site, Brooks Range Foothills, Alaska. *Ecography (Cop.)* **12**, 238–261 (1989).
31. López Martínez, J. et al. Geomorphology and surface landforms distribution in selected ice-free areas in the South Shetland Islands, northern Antarctic peninsula region. (2016).
32. López-Martínez, J., Serrano, E., Schmid, T., Mink, S. & Linés, C. Periglacial processes and landforms in the South Shetland Islands (northern Antarctic Peninsula region). *Geomorphology* **155–156**, 62–79 (2012).
33. Francelino, M. R. et al. Geomorphology and soils distribution under paraglacial conditions in an ice-free area of Admiralty Bay, King George Island, Antarctica. *Catena* **85**, 194–204 (2011).
34. Vera, M. L. Colonization and demographic structure of *Deschampsia antarctica* and *Colobanthus quitensis* along an altitudinal gradient on Livingston Island, South Shetland Islands, Antarctica. *Polar Res* **30**, 7146 (2011).
35. Simas, F. N. B. et al. Ornithogenic cryosols from Maritime Antarctica: Phosphatization as a soil forming process. *Geoderma* **138**, 191–203 (2007).
36. Thomazini, A. et al. Geospatial variability of soil CO<sub>2</sub>–C exchange in the main terrestrial ecosystems of Keller Peninsula, Maritime Antarctica. *Sci. Total Environ.* **562**, 802–811 (2016).
37. de Sá Mendonça, E., La Scala, N., Panosso, A. R., Simas, F. N. B. & Schaefer, C. E. G. R. Spatial variability models of CO<sub>2</sub> emissions from soils colonized by grass (*Deschampsia antarctica*) and moss (*Sanionia uncinata*) in Admiralty Bay, King George Island. *Antarct. Sci.* **23**, 27–33 (2011).
38. Zhu, R., Bao, T., Wang, Q., Xu, H. & Liu, Y. Summertime CO<sub>2</sub> fluxes and ecosystem respiration from marine animal colony tundra in maritime Antarctica. *Atmos. Environ.* **98**, 190–201 (2014).
39. Sindel, B. M. et al. Ecology and management of invasive plants in the sub-Antarctic and Antarctic regions: evidence and synthesis from Macquarie Island. *Plant Ecol. Divers.* **15**, 183–198 (2022).
40. Boy, J. et al. Successional patterns along soil development gradients formed by glacier retreat in the Maritime Antarctic, King George Island. *Rev. Chil. Hist. Nat.* **89**, 1–17 (2016).
41. Losapio, G. et al. The consequences of glacier retreat are uneven between plant species. *Front. Ecol. Evol.* **8**, 616562 (2021).
42. Badenhauer, I. et al. Do non-native plants affect terrestrial arthropods in the sub-Antarctic Kerguelen Islands? *Polar Biol* **45**, 491–506 (2022).
43. Song, J. et al. A meta-analysis of 1,119 manipulative experiments on terrestrial carbon-cycling responses to global change. *Nat. Ecol. Evol.* **3**, 1309–1320 (2019).
44. Terrer, C. et al. A trade-off between plant and soil carbon storage under elevated CO<sub>2</sub>. *Nature* **591**, 599–603 (2021).
45. Tang, J. & Baldocchi, D. D. Spatial-temporal variation in soil respiration in an oak–grass savanna ecosystem in California and its partitioning into autotrophic and heterotrophic components. *Biogeochemistry* **73**, 183–207 (2005).
46. Cavieres, L. A. et al. Ecophysiological traits of Antarctic vascular plants: their importance in the responses to climate change. *Plant Ecol* **217**, 343–358 (2016).
47. Strauss, S. L., Ruhland, C. T. & Day, T. A. Trends in soil characteristics along a recently deglaciated foreland on Anvers Island, Antarctic Peninsula. *Polar Biol* **32**, 1779–1788 (2009).
48. Cannone, N., Malfasi, F., Favero-Longo, S. E., Convey, P. & Guglielmin, M. Acceleration of climate warming and plant dynamics in Antarctica. *Curr. Biol.* **32**, 1599–1606 (2022).
49. Robinson, S. A. et al. Rapid change in East Antarctic terrestrial vegetation in response to regional drying. *Nat. Clim. Chang.* **8**, 879–884 (2018).
50. Amesbury, M. J. et al. Widespread biological response to rapid warming on the Antarctic Peninsula. *Curr. Biol.* **27**, 1616–1622 (2017).
51. Peña, M. F. et al. Have historical climate changes affected Gentoo penguin (*Pygoscelis papua*) populations in Antarctica? *PLoS One* **9**, e95375 (2014).
52. Sander, M., Balbão, T. C., Costa, E. S., Santos, C. R. D. & Petry, M. V. Decline of the breeding population of *Pygoscelis antarctica* and *Pygoscelis adeliae* on Penguin Island, South Shetland, Antarctica. *Polar Biol* **30**, 651–654 (2007).
53. Simas, F. N. B. et al. Organic carbon stocks in permafrost-affected soils from Admiralty Bay, Antarctica. *US Geol. Surv. Natl. Acad. USGS OF-2007-1047, Short Res. Pap.* **76**, (2007).
54. Ping, C. L., Jastrow, J. D., Jorgenson, M. T., Michaelson, G. J. & Shur, Y. L. Permafrost soils and carbon cycling. *Soil* **1**, 147–171 (2015).
55. Fontaine, S. et al. Stability of organic carbon in deep soil layers controlled by fresh carbon supply. *Nature* **450**, 277–280 (2007).
56. Olsson, L. et al. in *IPCC Special Report on Climate Change, Desertification, Land 5 Degradation, Sustainable Land Management, Food Security, and 6 Greenhouse Gas Fluxes in Terrestrial Ecosystems* 1 (Intergovernmental Panel on Climate Change (IPCC), 2019).
57. Pörtner, H.-O. et al. IPCC special report on the ocean and cryosphere in a changing climate. *IPCC Intergov. Panel Clim. Chang. Geneva, Switz.* **1**, 1–755 (2019).
58. Daher, M. et al. Ornithogenic soils on basalts from maritime Antarctica. *CATENA* **173**, 367–374 (2019).
59. Pires, C. V. et al. Soil organic carbon and nitrogen pools drive soil C-CO<sub>2</sub> emissions from selected soils in Maritime Antarctica. *Sci. Total Environ.* **596–597**, 124–135 (2017).
60. Gautam, S. et al. Continental United States may lose 1.8 petagrams of soil organic carbon under climate change by 2100. *Glob. Ecol. Biogeogr.* **31**, 1147–1160 (2022).
61. Wang, M. et al. Global soil profiles indicate depth-dependent soil carbon losses under a warmer climate. *Nat. Commun.* **13**, 5514 (2022).
62. Wang, M. et al. Responses of soil organic carbon to climate extremes under warming across global biomes. *Nat. Clim. Chang.* 1–8 (2023).
63. Moraes, A. G. et al. Environmental correlation and spatial autocorrelation of soil properties in Keller Peninsula, Maritime Antarctica. *Rev. Bras. Ciência do Solo* **41**, (2018).
64. Navas, A. et al. Soil characteristics on varying lithological substrates in the South Shetland Islands, maritime Antarctica. *Geoderma* **144**, 123–139 (2008).
65. Tisdall, J. M. & Oades, J. M. Organic matter and water-stable aggregates in soils. *J. soil Sci.* **33**, 141–163 (1982).
66. Six, J., Conant, R. T., Paul, E. A. & Paustian, K. Stabilization mechanisms of soil organic matter: implications for C-saturation of soils. *Plant Soil* **241**, 155–176 (2002).



67. Blumel, W. D. & Eitel, B. Geocological aspects of maritime-climatic and continental periglacial regions in Antarctica (South Shetlands, Antarctic Peninsula and Victoria Land). *Geökodynamic* **10**, 201–214 (1989).
68. Convey, P. et al. Global southern limit of flowering plants and moss peat accumulation. *Polar Res* **30**, 8929 (2011).
69. Van Lipzig, N. P. M., King, J. C., Lachlan-Cope, T. A. & Van den Broeke, M. R. Precipitation, sublimation, and snow drift in the Antarctic Peninsula region from a regional atmospheric model. *J. Geophys. Res. Atmos.* **109**, (2004).
70. Schmitz, D. et al. Diversity and species associations in cryptogam communities along a pedoenvironmental gradient on Elephant Island, Maritime Antarctica. *Folia Geobot* **55**, 211–224 (2020).
71. Poelking, E. L., Schaefer, C. E. R., Fernandes Filho, E. I., de Andrade, A. M. & Spielmann, A. A. Soil–landform–plant–community relationships of a periglacial landscape on Potter Peninsula, maritime Antarctica. *Solid Earth* **6**, 583–594 (2015).
72. Smellie, J. L., Hunt, R. J., McIntosh, W. C. & Esser, R. P. Lithostratigraphy, age and distribution of Eocene volcanic sequences on eastern king george island, South Shetland islands, Antarctica. *Antarct. Sci.* **33**, 373–401 (2021).
73. Smellie, J. L., McIntosh, W. C., Whittle, R., Troedson, A. & Hunt, R. J. A lithostratigraphical and chronological study of Oligocene–Miocene sequences on eastern King George Island, South Shetland Islands (Antarctica), and correlation of glacial episodes with global isotope events. *Antarct. Sci.* **33**, 502–532 (2021).
74. Smellie, J. L., Pankhurst, R. J., Thomson, M. R. A. & Davies, R. E. S. The geology of the South Shetland Islands: VI. Stratigraphy, geochemistry and evolution. *Sci. Rep. - British Antarctic Survey* **87**, (1984).
75. Pirrie, D. Petrography and provenance of the Marambio Group, Vega Island, Antarctica. *Antarct. Sci.* **6**, 517–527 (1994).
76. Nelson, P. N. H. The James Ross Island Volcanic Group of north-east Graham Land. (1966).
77. Zinsmeister, W. J. Review of the Upper Cretaceous–Lower Tertiary sequence on Seymour Island, Antarctica. *J. Geol. Soc. London.* **139**, 779–785 (1982).
78. Mello, D. C. et al. Radiometric and magnetic susceptibility characterization of soil profiles: Geophysical data and their relationship with Antarctic periglacial processes, pedogenesis, and lithology. *CATENA* **232**, 107427 (2023).
79. FAO. *World reference base for soil resources 2014. International soil classification system for naming soils and creating legends for soil maps. World Soil Resources Reports No. 106.* <https://doi.org/10.1017/S0014479706394902> (2014).
80. Dane, J. H. & Toppp, C. G. *Methods of soil analysis, Part 4: Physical methods.* **20**, (John Wiley & Sons, 2020).
81. Abdelbaki, A. M. Evaluation of pedotransfer functions for predicting soil bulk density for U.S. soils. *Ain Shams Eng. J* **9**, 1611–1619 (2018).
82. Al-Shammary, A. A. G. et al. Soil bulk density estimation methods: A review. *Pedosphere* **28**, 581–596 (2018).
83. de Mello, D. C. et al. A new methodological framework for geophysical sensor combinations associated with machine learning algorithms to understand soil attributes. *Geosci. Model Dev.* **15**, 1219–1246 (2022).
84. de Mello, D. C. et al. Chemical weathering detection in the periglacial landscapes of Maritime Antarctica: New approach using geophysical sensors, topographic variables and machine learning algorithms. *Geoderma* **438**, (2023).
85. Bottai, M., Kim, T., Lieberman, B., Luta, G. & Peña, E. On optimal correlation-based prediction. *Am. Stat.* **76**, 313–321 (2022).
86. O'Brien, L. Mpspline2: mass-preserving spline functions for soil data. (2022).
87. Beaudette, D., Roudier, P., Beaudette, M. D. & RColorBrewer, M. Package 'aqp'. (2022).
88. Howat, I. M., Porter, C., Smith, B. E., Noh, M.-J. & Morin, P. The reference elevation model of Antarctica. *Cryosph* **13**, 665–674 (2019).
89. Brenning, A., Bangs, D., Becker, M., Schratz, P. & Polakowski, F. Package 'RSAGA'. *Compr. R Arch. Netw.* <https://CRAN.R-project.org/package=RSAGA> (2018).
90. Karger, D. N. et al. Climatologies at high resolution for the earth's land surface areas. *Sci. data* **4**, 1–20 (2017).
91. Warszawski, L. et al. The inter-sectoral impact model intercomparison project (ISI-MIP): project framework. *Proc. Natl. Acad. Sci.* **111**, 3228–3232 (2014).
92. Cook, B. I. et al. Twenty-first century drought projections in the CMIP6 forcing scenarios. *Earth's Futur.* **8**, e2019EF001461 (2020).
93. Hijmans, R. J. et al. Package 'terra'. *Maint. Vienna, Austria* (2022).
94. Meinshausen, N. Quantregforest: quantile regression forests. *R Packag. version 1–3* (2017).
95. Kuhn, M. Caret: classification and regression training. *Astrophys. Source Code Libr.* ascl-1505 (2022).
96. R. Core Team. R: A language and environment for statistical computing. (2023).
97. Fernandes Filho, E. I. labgeo: Collection of Functions to Fit Models with Emphasis in Land Use and Soil Mapping. R Package Version 0.3.9.3. Available online: <https://github.com/elpidiofilho/labgeo>. (2019).

## Acknowledgements

We express our gratitude to the National Council for Scientific and Technological Development (CNPq) for providing the first author's scholarship and essential resources through grants No. 134608/2015-1 and 305996/2018-5. Additionally, we acknowledge partial funding for this study from the Coordenação de Aperfeiçoamento de Pessoal de Nível Superior - Brazil (CAPES) - Finance Code 001. We extend our thanks to the Terrantar - UFV group, Geotechnologies in Soil Science group, Laboratório de Pedometria e Geoprocessamento (LabGeo - UFV), 'Programa de Pós-Graduação em Solos e Nutrição de Plantas - PGSNP' of the Soil Department of the Universidade Federal de Viçosa, Brazil, and Programa Antártico Brasileiro (PROANTAR) for their valuable support. We also extend our gratitude to Fundação de Amparo a Pesquisa do Estado de São Paulo (FAPESP) for the scholarship awarded to the first author (project 2024/06285-1), which enabled the completion of this manuscript at another institution (ESALQ/USP). The methodology developed in this work will be applied to mangrove areas in the study titled 'Impact of Global Warming on the Dynamics of Soil Organic Carbon Stocks in the Mangrove Ecosystem: Assessment of Climate Change Feedbacks'. We also appreciate the Instituto Nacional de Ciência e Tecnologia da Criosfera (INCT da Criosfera) Brazil for the financial and material support, and Cluster - UFV for processing support.

## Author contributions

Mello, D.C. conceived the study, conducted interpretation and analyses, and developed the manuscript and led the revision-writing of the manuscript with input from all authors. Moquedace, C.M. and Baldi, C.G. performed the model simulations, validation, and statistical analysis. Silva, L.V. and Veloso, G.V. prepared the figures. Siqueira, R.G. prepared the dataset and tabulate the data for modeling process. Francelino, M. R. and Schaefer, C.E. G.R provided financial support and resources and the supervision of this study. Veloso, G. V., Tiago O. Ferreira, Lucas C. Gomes, Thomazini, A., Fernandes-Filho, E. I., Senra, E. O. and Demattê, J.A. M. revised the manuscript and methods.

## Competing interests

The authors declare no competing interests.

## Additional information

**Supplementary information** The online version contains supplementary material available at <https://doi.org/10.1038/s43247-024-01937-z>.

**Correspondence** and requests for materials should be addressed to Márcio R. Francelino.

**Peer review information** *Communications Earth & Environment* thanks Susana del Carmen Fernández Menéndez and the other, anonymous, reviewer(s) for their contribution to the peer review of this work. Primary Handling Editors: Alice Drinkwater. A peer review file is available.

**Reprints and permissions information** is available at <http://www.nature.com/reprints>

**Publisher's note** Springer Nature remains neutral with regard to jurisdictional claims in published maps and institutional affiliations.

**Open Access** This article is licensed under a Creative Commons Attribution 4.0 International License, which permits use, sharing, adaptation, distribution and reproduction in any medium or format, as long as you give appropriate credit to the original author(s) and the source, provide a link to the Creative Commons licence, and indicate if changes were made. The images or other third party material in this article are included in the article's Creative Commons licence, unless indicated otherwise in a credit line to the material. If material is not included in the article's Creative Commons licence and your intended use is not permitted by statutory regulation or exceeds the permitted use, you will need to obtain permission directly from the copyright holder. To view a copy of this licence, visit <http://creativecommons.org/licenses/by/4.0/>.

© The Author(s) 2025